Biomedical Signal Processing and Control xxx (2013) xxx–xxx

Contents lists available at SciVerse ScienceDirect

Biomedical Signal Processing and Control

journal homepage: www.elsevier.com/locate/bspc

# Catheter ablation outcome prediction in persistent atrial fibrillation using weighted principal component analysis

Marianna Meo[a,*], Vicente Zarzoso[a], Olivier Meste[a], Decebal G. Latcu[b], Nadir Saoudi[b]

[a] Laboratoire d'Informatique, Signaux et Systèmes de Sophia Antipolis (I3S), Université Nice Sophia Antipolis, CNRS, France
[b] Service de Cardiologie, Centre Hospitalier Princesse Grace, Monaco

ARTICLE INFO

*Article history:*
Received 22 June 2012
Received in revised form 1 February 2013
Accepted 11 February 2013
Available online xxx

*Keywords:*
Atrial fibrillation (AF)
Catheter ablation (CA)
Electrocardiogram (ECG)
Spatial diversity
Weighted principal component analysis (WPCA)

ABSTRACT

Radiofrequency catheter ablation (CA) is increasingly employed to treat persistent atrial fibrillation (AF), yet selection of patients who would positively respond to this therapy is currently a critical problem. Several parameters of the surface 12-lead electrocardiogram (ECG) have been analyzed in previous works to predict AF termination by CA. Nevertheless, they are affected by some limitations, such as manual computation and the examination of a single ECG lead while neglecting contributions from other electrodes. AF spatio-temporal organization has been described on surface ECG by means of the normalized mean square error (NMSE) between consecutive atrial activity (AA) signal segments and their reduced-rank approximations based on principal component analysis (PCA). However, these features do not show to be correlated with CA outcome. In this study, such descriptors are adequately adapted and applied to CA outcome prediction. An NMSE index is put forward, computed over the set of eight linearly independent ECG leads after AA signal rank-1 approximations determined by weighted principal component analysis (WPCA). The final predictor is able to discriminate between successful ($70.76 \pm 17.74$) and failing CA procedures ($37.54 \pm 20.01$) before performing the ablation ($p$-value = 0.0013, AUC = 0.91). The proposed WPCA-based technique emphasizes the most descriptive components of AF electrophysiology by selectively enhancing contributions coming from the most representative ECG leads. Our investigation confirms that ECG spatial diversity exploitation in this WPCA-based framework not only endows the NMSE index with clinical value in the context of CA outcome prediction, but it also improves classification accuracy and increases robustness to ECG lead selection.



## 1. Introduction

Atrial fibrillation (AF) is a sustained cardiac arrhythmia characterized by rapid and disorganized atrial activations inducing a loss of atrial mechanical efficacy. Several theories have been suggested to explain AF electrophysiological mechanisms, so as to put forth a systematic procedural protocol for its treatment. AF activity has been first regarded as the result of interactions between multiple wandering atrial wavelets [1,2]. On the other hand, it is commonly acknowledged that pulmonary veins (PVs) significantly contribute to AF maintenance and evolution, especially in paroxysmal forms of this disease [3]. In spite of major advances in its treatment, AF remains a significant cause of cardiovascular morbidity and mortality, especially those arising from stroke and heart failure.

Radiofrequency catheter ablation (CA) has become the first-line strategy [4] for the treatment of this disease. However, as the precise pathophysiology of AF dynamics has not been completely clarified yet, it is still questionable whether CA effectively suppresses abnormal rhythm sources, and how it affects heart electrical substrate. Different CA techniques have been developed, yet none of them is widely considered as effective for the treatment of persistent AF. Their performance is still far from satisfactory, and they are less effective than equivalent procedures for paroxysmal AF. Since this cardiac interventional procedure is profoundly influenced by operator's experience and patient's health conditions, results reported by clinical centers are quite disparate and not easily comparable [5–7]. It follows that its efficacy in terminating AF and avoiding its recurrence is not guaranteed for all patients. This situation explains the increasing tendency to attempt an a priori selection of patients who can undergo CA and experience durable sinus rhythm (SR) restoration. Several parameters extracted from the surface ECG have been proposed as potential predictors of CA outcome [8,9]. For example, prolongation of atrial fibrillation cycle length (AFCL) can be associated with AF termination by CA [10]. In other studies [8], it has been argued that the higher the amplitude

* Corresponding author. Tel.: +33 492942741.
*E-mail addresses:* meo@i3s.unice.fr (M. Meo), zarzoso@i3s.unice.fr (V. Zarzoso), meste@i3s.unice.fr (O. Meste), dglatcu@yahoo.com (D.G. Latcu), nsaoudi@chpg.mc (N. Saoudi).

1746-8094/$ – see front matter © 2013 Elsevier Ltd. All rights reserved.
http://dx.doi.org/10.1016/j.bspc.2013.02.002

of the fibrillatory waves (f-waves) observed on the surface ECG, the more likely procedural success.

In parallel, another line of research aims at noninvasive measures of AF spatio-temporal complexity, with the underlying assumptions that treatment modalities should be chosen and therapy outcome could be predicted on the basis of these measures. In [11], a noninvasive measure of AF organization is assessed by the normalized mean square error (NMSE) values between the atrial activity (AA) signal and its rank-3 approximations determined by principal component analysis (PCA) in lead $V_1$ [11]. This argument is supported by the hypothesis of a correlation between AF organization and the number and interactions of atrial wavefronts through the heart substrate. The choice of $V_1$ is justified by the fact that it presents the maximum atrial-to-ventricular amplitude ratio among all ECG leads [12]. In [13], CA performance was shown to influence AF spatio-temporal organization, and its effect can be quantified by variations in NMSE values.

Nevertheless, such parameters are affected by several shortcomings. In the first place, some classical ECG-based descriptors are manually computed [8,10], so they are subject to operators' subjectivity and thus prone to errors. Furthermore, as most of them are measured in only one ECG lead, they do not account for information that may be provided by other electrodes. Indeed, ECG analysis is not always straightforward, and visual inspection does not capture AF features underlying the whole ensemble of leads; hence, the limitations of classical single-lead techniques, which do not fully exploit multilead ECG spatial diversity. However, AF spatio-temporal complexity as defined in [11] has not been shown to correlate with CA outcome.

Our investigation focuses on the potential application of the spatio-temporal organization of AA measured on the standard ECG by the NMSE index as a tool to discriminate between successful and failing CA procedures before applying the therapy. Contributions provided from the eight independent ECG leads are expressed in terms on NMSE between successive segments of the actual AA signal and their rank-1 approximations computed by weighted principal component analysis (WPCA), and they are finally combined in a single parameter capable of predicting long-term CA outcome. Thanks to this decomposition, the spatial variability of the standard ECG is taken into account, and the most significant ECG leads are also automatically enhanced by assigning different weights to data based on their estimated relevance.

## 2. Methods

### 2.1. Characteristics and acquisition modalities of the persistent-AF database

Twenty patients (19 males, $60 \pm 11$ years) with a median persistent AF episode duration of 4.5 months (2–84) were enrolled in the present study. They all underwent CA at the Cardiology Department of Princess Grace Hospital in Monaco, performed with the aid of Prucka Cardiolab and Biosense CARTO electrophysiology measurement systems. They all gave their informed consent. Surface 12-lead ECG recordings were acquired at the beginning of the procedure, at a sampling rate of 1 kHz. An example of the signal recorded on the lead $V_1$ for one of the patients is shown in Fig. 1. CA was accomplished according to the sequential stepwise protocol [14], whose major actions consist in 1) circumferential PV isolation, 2) fragmented potentials' ablation, and 3) non-PV triggers, roof line and mitral isthmus line right atrial ablation.

The most recent HRS Expert Consensus Statement guidelines for CA trials [14] recommend that immediately after CA performance, there is a three-month "blanking period" during which any fibrillatory episodes are not regarded as symptoms of AF recurrence, but as a physiological reaction during recovery from CA. After this blanking period, if the patient remains free of arrhythmia recurrences, procedural AF termination is considered effectively accomplished.

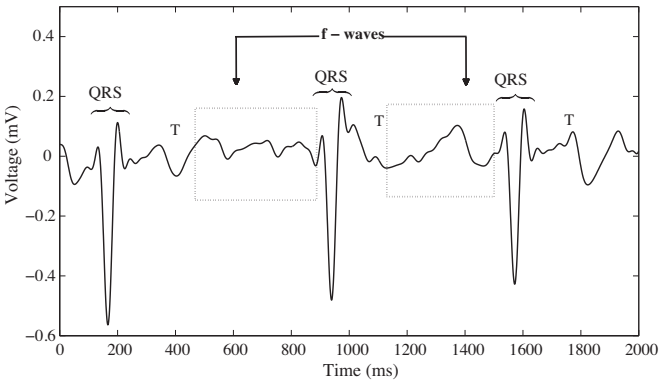


**Fig. 1.** Example of ECG recording during AF and its characteristic waves. Boxes highlight TQ intervals which are concatenated to form the AA signal $\mathbf{Y}_{AA}$ in Eq. (1).

Procedural success is defined as freedom from ECG/Holter documented sustained AF recurrence (>30 s) during follow-up, after the 3-month blanking period. Immediately after performing CA, AF can be converted either directly to SR or to intermediate tachyarrhythmia, exclusively by ablation or after an electrical cardioversion. For its clinical interest, a long-term criterion is adopted in our investigation to distinguish between successful and ineffective CA procedures. In our experimental framework, after a median follow-up of 9.5 months, CA was successfully accomplished in $n_S = 13$ out of $n_P = 20$ patients (65%), whereas $n_F = 7$ procedures were not effective. A follow-up of $m$ months was available at the time of our analysis, where $m$ ranged between 4 and 19 months depending on the patient.

Some patients received a pharmacological treatment subsequent to CA procedure, mainly amiodarone (for some patients, solatol and flecaine). Three patients underwent a second ablation. In this case, only ECG signals related to the first procedure are taken into account in our study. As opposed to previous studies [8,9], termination of AF during CA was not achieved in all patients. Nevertheless, this is not detrimental to our analysis, since AF termination by CA is not predictive of long-term outcome [15], which is the event with clinical interest.

### 2.2. ECG preprocessing and atrial activity segmentation

A fourth-order zero-phase Chebyshev type II bandpass filter with −3 dB attenuation band between 0.5 Hz and 30 Hz has been applied to standard ECG recordings of our database, whose length is about 1 min. This preprocessing stage allows AF content enhancement, whose dominant frequency typically ranges between 3 and 12 Hz, as well as removal of baseline wandering and high frequency noise such as myoelectric artifacts and 50 Hz power line interference. Automatic detection of ECG fiducial points is then accomplished, in order to segment TQ intervals. R wave time instants are detected on lead $V_1$ using the Pan–Tompkins' algorithm [16]. Then, Q wave onset is defined 40 ms before the subsequent R wave, this being the typical duration of this wave in these conditions (an abnormal Q wave denotes presence of infarct). Finally, T wave offset is identified with an improved version of Woody's method and automatically computed after visual inspection and selection of the lead exhibiting the most visible T waves (in general, $V_2$ and $V_3$) [17]. Such intervals are finally mean-corrected and

Please cite this article in press as: M. Meo, et al., Catheter ablation outcome prediction in persistent atrial fibrillation using weighted principal component analysis, Biomed. Signal Process. Control (2013), http://dx.doi.org/10.1016/j.bspc.2013.02.002

concatenated, so obtaining the $(L \times N)$ data matrix $\mathbf{Y}_{AA}$ representing AA content only:

$$\mathbf{Y}_{AA} = [\mathbf{y}_{AA}(1) \cdots \mathbf{y}_{AA}(N)] \in \mathbb{R}^{L \times N} \quad (1)$$

where vector $\mathbf{y}_{AA}(t) = [y_1(t), \ldots, y_L(t)]^T$ represents the multilead AA signal at the sample index $t$, $L$ stands for the number of leads used, and $N$ the number of samples of the AA signal $y_\ell(n)$ for each lead $\ell$=1, 2, ..., $L$.

The redundancy in ECG leads [18] prompted us to discard lead III and Goldberger's augmented leads ($aV_R$, $aV_L$, $aV_F$), since leads I and II can fully characterize heart electrical activity on the frontal plane. Finally, all precordial leads have been introduced too, in order to record the electric potential changes in the heart in a cross-sectional plane. This yields a total of $L = 8$ leads, that is, I, II, $V_1$–$V_6$.

### 2.3. Atrial activity complexity

Several parameters describing different aspects of AF spatio-temporal organization have been proposed and analyzed in previous works, according to various definitions of this concept. The rationale is to investigate evidences of some underlying structure in atrial activity during AF. The wide variety of different criteria that have been proposed in the literature makes it difficult to compare and interpret all such indices.

The degree of organization of AF wavefronts propagating inside the atria has been traditionally examined on intracardiac recordings. In [19] the level of spatial correlation between multiple activation sequences is correlated with AF presence, and enables selection of antiarrhythmic drug therapy for SR maintenance. In [20], AF morphology characterization based on PCA and automatic clustering provides a quantitative tool for AF classification. The study described in [21] also proposes more advanced techniques for feature extraction and SVM-classification to perform the same task. Other approaches focus on temporal regularity of atrial activations and assess AF complexity according to the level of beat-to-beat variability [22]. More recently, time-frequency analysis has been applied to endocavitarian recordings in [23]. Despite their effectiveness, such strategies are all quite invasive and do not provide a priori predictions of CA outcome.

By contrast, noninvasive recordings can easily provide measures of heart electrical activity. Some nonlinear measures based on sample entropy [24] computed on surface ECG have also been exploited to predict spontaneous paroxysmal AF termination [25]. In [26], it is also stated that more organized AF patterns as quantified by this index predict AF termination by electrical cardioversion. The main drawback of these indices is that they are computed in only one ECG lead, thus potential information about AF complexity provided by the remaining leads is not exploited.

Recent attempts to exploit ECG spatial properties have been made in [27] by combining frequency and complexity measures, allowing the distinction between persistent and long-standing AF. Also, in [28] wavefront propagation maps extracted on BSPM recordings have been used for visual classification of AF complexity types according to Konings' criteria [1] on BSPM recordings. Based on this approach, a quantitative multilead analysis is carried out in [11]. This study underlines that AA spatio-temporal organization can be effectively represented by the first few principal components (PCs) determined by PCA, retaining most of the total variance, by quantifying the similarity between the principal subspaces of the AA signal along consecutive time segments. For sake of completeness, the mathematical description of this complexity measure is summarized next, as it constitutes an important ingredient of the present work.

The multilead AA signal $\mathbf{Y}_{AA}$ is split into $S$ equal-length segments, each containing $N_S = [N/S]$ samples, so that $\mathbf{Y}_{AA} = [\mathbf{Y}^{(1)}, \mathbf{Y}^{(2)}, \ldots, \mathbf{Y}^{(S)}]$, with $\mathbf{Y}^{(s)} = [\mathbf{y}((s-1)N_S+1), \mathbf{y}((s-1)N_S+2), \ldots, \mathbf{y}(sN_S)]$, $s = 1, \ldots, S$. The AA signal $\mathbf{Y}^{(r)}$ is examined in a certain reference segment $r \neq s$ and decomposed by PCA according to the linear model $\mathbf{Y}^{(r)} = \mathbf{M}^{(r)}\mathbf{X}^{(r)}$, $r = 1$ in [11]. Subsequently, a fixed number $n$ of columns $\mathbf{M}_n^{(r)}$ is extracted from the mixing matrices computed by PCA in this reference interval. Such columns, the so-called principal directions, weight the relative spatial contribution of the PCs to the ECG leads. After these steps, the AA signal is estimated in all other segments $s \neq r$ by projecting $\mathbf{Y}^{(s)}$ on the subspace spanned by the columns of $\mathbf{M}_n^{(r)}$, thus yielding:

$$\mathrm{Y}_n^{(s,r)} = \mathbf{M}_n^{(r)}[\mathbf{M}_n^{(r)T}\mathbf{M}_n^{(r)}]^{-1}\mathbf{M}_n^{(r)T}\mathbf{Y}^{(s)} \quad (2)$$

that is, the orthogonal projection of $\mathbf{Y}^{(s)}$ on the span of $\mathbf{M}_n^{(r)}$. Hence, the approximation quality can be evaluated by means of the normalized mean square error $\mathrm{NMSE}_{\ell,n}^{(s,r)}$ between the input signal $y_\ell^{(s)}(t)$ on the $\ell$th lead and its projection $\hat{y}_{\ell,n}^{(s,r)}(t)$ found in the $\ell$th row of Eq. (2):

$$\mathrm{NMSE}_{\ell,n}^{(s,r)} = \frac{\sum_{t=1}^{N}[y_\ell^{(s)}(t) - \hat{y}_{\ell,n}^{(s,r)}(t)]^2}{\sum_{t=1}^{N}[y_\ell^{(s)}(t)]^2} \quad (3)$$

with $\ell$=1, ⋯, $L$. In [11], the mean NMSE is computed by assuming the first segment as a reference ($r = 1$), and averaging Eq. (3) over the remaining segments ($s = 2, \ldots, S$).

Nonetheless, in [11] the NMSE introduced in Eq. (3) is merely computed on a single lead, so spatial variability typical of multilead recordings is not entirely exploited. In particular, despite the proximity of lead $V_1$ to the right atrial free wall, there is the risk of not considering further useful information provided by other ECG leads. In addition, as all aforementioned parameters, this single-lead index proved unable to predict CA outcome [13].

In order to render a more general perspective of AF complexity over all leads and provide the NMSE index with further clinical value with respect to CA outcome prediction, several alternative strategies have been put forward. In [29] some statistical descriptors combining NMSE contributions from several ECG leads depending on AA signal variance were able to assess the level of spatio-temporal repetitiveness of the AA signal during several steps of the ablation and predict its outcome. NMSE computation was repeated for each segment, for all possible combinations between estimated and reference segments $r$, $s = 1, \ldots, S$, with $r \neq s$. The analysis presented in [30] puts forward the computation of reduced-rank representations of AF complexity measures by means of the nonnegative matrix factorization (NMF). Despite their advantages, these strategies prove effective only in short-term prediction, so they are not able to render the mechanisms of electrical remodeling of the heart substrate altered by CA over longer follow-up periods and discriminate between the classes of interest. Results from these works encouraged us to design a more robust methodology capable of selectively emphasizing the most relevant contributions from ECG observations to improve classification accuracy in the CA outcome prediction context. More precisely, we aim at characterizing the NMSE index in a multilead framework so as to predict CA outcome by applying the weighted PCA of the atrial signal matrix.

### 2.4. Weighted principal component analysis

As mentioned in the previous section, a possible strategy aiming at the exploitation of the multivariate properties of the standard ECG consists in searching for a reduced set of uncorrelated components retaining as much of its spatial variability as possible. In order to achieve this objective, PCA has been widely applied to the ECG, due to its non-parametric nature, simplicity of implementation and

Please cite this article in press as: M. Meo, et al., Catheter ablation outcome prediction in persistent atrial fibrillation using weighted principal component analysis, Biomed. Signal Process. Control (2013), http://dx.doi.org/10.1016/j.bspc.2013.02.002

versatility [31–34]. However, PCA is sometimes not recommended in ECG processing. As it gives the same relevance to all observations, the low-rank representation tends to be quite sensitive to outliers and can become unstable. This issue affects every decomposition method based on the minimization of a criterion function in the ordinary least squares (OLS) sense. To avoid these limitations, we put forward a more robust multivariate analysis aiming at decomposing the multilead AA signal defined in Eq. (1) and split into $S$ segments.

The approach proposed is the *weighted principal component analysis (WPCA)*, fitting the data model $\mathbf{Y}^{(r)}$ by minimizing a weighted least squares (WLS) loss function [35] as in the scheme described next. According to the WLS approach, each entry of the input matrix $\mathbf{Y}^{(r)}$ defined in a reference segment $r$ is separately weighted with a fixed, nonnegative quantity. These leveraging factors can be collected in a matrix $\mathbf{W}^{(r)}$ having the same dimensions as $\mathbf{Y}^{(r)}$. The general form of the WLS loss function can be written as:

$$h(\mathbf{Y}^{(r)}|\mathbf{Y}^{(r)}, \mathbf{W}^{(r)}) = \|(\mathbf{Y}^{(r)} - \mathbf{Y}^{(r)}) * \mathbf{W}^{(r)}\|_{\mathrm{F}}^2 = \sum_{\ell=1}^{L}\sum_{m=1}^{N}[w_{\ell,m}^{(r)}(y_{\ell,m}^{(r)} - \hat{y}_{\ell,m}^{(r)})]^2 \quad (4)$$

where * denotes the Hadamard (or elementwise) product, whereas the operator $\|\cdot\|_{\mathrm{F}}$ stands for the Frobenius norm. In our experimental framework, the output model $\mathrm{Y}^{(r)} = \mathbf{M}^{(r)}\mathbf{X}^{(r)}$ consists of the WPCA vectors contained in the $L \times n$ matrix $\mathbf{M}^{(r)}$, and the $n \times N_S$ matrix $\mathbf{X}^{(r)}$ representing the PCs, stored in decreasing order of variance. As in classical PCA, some orthogonality constraints are imposed on $\mathbf{M}^{(r)}$ and $\mathbf{X}^{(r)}$ in order to reduce the ambiguities in the model.

### 2.5. Assignment of the weight matrix

Special consideration must be paid to the assignment of the weights collected in matrix $\mathbf{W}^{(r)}$. Indeed, an accurate choice of these values can give rise to a kind of filtering action which enhances not only the leads, but also the time samples giving the most content-bearing contributions while discarding those that do not yield significant information or can pollute atrial observations. In our application, all temporal samples on the same lead are equally treated. Also, we aim at emphasizing leads with more stable and regular waveforms while reducing the influence of those characterized by higher temporal dispersion, quantified in terms of energy. We assume that the input signal $\mathbf{Y}^{(r)}$ can be modeled as:

$$\mathbf{Y}^{(r)} = \mathbf{Y}_{\mathrm{S}}^{(r)} + \mathbf{Y}_{\mathrm{N}}^{(r)} \quad (5)$$

namely, as the sum of a meaningful component $\mathbf{Y}_{\mathrm{S}}^{(r)}$ (describing AF in our application) and a noisy component $\mathbf{Y}_{\mathrm{N}}^{(r)}$, due not only to data acquisition noise, but also to elements discarded by the reduced-rank WPCA-approximation. Our hypothesis is that $\mathbf{Y}_{\mathrm{N}}^{(r)} = (\mathbf{Y}^{(r)} - \mathbf{Y}_{\mathrm{S}}^{(r)})$ is characterized by a high degree of spatio-temporal variability which can alter or hide informative elements coming from $\mathbf{Y}_{\mathrm{S}}$ in each lead. This term can be regarded as the argument of the WLS criterion defined in Eq. (4) to be minimized according to the algorithm described in the sequel. Hence, one way of reducing its influence on the overall signal is by weighing each lead by the inverse of AA signal variance, thus giving more importance to the least powerful electrodes. As a result, each row of $\mathbf{W}^{(r)}$ is weighted by the inverse of the standard deviation $\sigma_{\ell}^{(r)}$ associated with the corresponding lead $\ell$=1, . . ., $L$ in $\mathbf{Y}^{(r)}$ and computed on each segment $r$ = 1, . . ., $S$:

$$\mathbf{W}^{(r)} = [(\sigma_1^{(r)})^{-1}(\sigma_2^{(r)})^{-1}\ldots(\sigma_L^{(r)})^{-1}]^T\mathbf{1} \quad (6)$$

where $\mathbf{1}$ is a row vector with $T$ unit entries. It is well worth noting that classical PCA is a special case of WPCA, where the elements of the weight matrix are all equal to 1. Once a weight matrix has been chosen, WPCA can be carried out using the algorithm summarized in the Appendix. Hence, the choice of decomposing each reference time interval in keeping with the WPCA model $\mathbf{Y}^{(r)} = \mathbf{M}^{(r)}\mathbf{X}^{(r)}$. In our application, this model is computed in each reference time interval. In such a context, AA signal estimation quality per segment is quantified by the NMSE defined in Eq. (3). Different weight matrices $\mathbf{W}^{(r)}$ will generally lead to different models $\mathbf{M}^{(r)}\mathbf{X}^{(r)}$, thus resulting in different NMSE values. The predictive value of different forms of $\mathbf{W}^{(r)}$ will be tested in Section 3.

### 2.6. Assessing atrial activity complexity from the NMSE values

After WPCA performance, we investigate how to properly combine NMSE values computed on each ECG lead and condense information in a unique predictor of CA outcome. With reference to Section 2.3, AF complexity evaluation in each segment is followed by the computation of the mean value $\mu_{\ell,n}$ and the standard deviation $\sigma_{\ell,n}$ of the NMSE in Eq. (3) over all possible combinations of estimated and reference segments ($s$, $r$), for each lead $\ell$ [29]. Parameter $\mu_{\ell,n}$ assesses global segment estimation performance, whereas $\sigma_{\ell,n}$ quantifies AF organization inter-segment variability. Finally, contributions from all leads analyzed are combined into the interlead NMSE weighted sum:

$$\widetilde{\mu}_n = \sum_{\ell=1}^{L}\frac{\mu_{\ell,n}}{\sigma_{\ell,n}^2}\Big/\sum_{\ell=1}^{L}\frac{1}{\sigma_{\ell,n}^2} \quad (7)$$

whose weights are represented by NMSE inverse variance values $1/\sigma_{\ell,n}^2$ per lead; contributions coming from ECG leads rendering more regular and less dispersive patterns are considered to be more relevant. A further interpretation of $\sigma_{\ell,n}$ can be given in terms of uncertainty: low values of this parameter depict a more stable reconstruction across time segments, whereas high values denote higher projection error uncertainty. Accordingly, leads guaranteeing a more robust AA content characterization have a stronger influence in the computation of the output descriptor. The choice of such weights can be further justified if we consider that the complexity information is reflected on the ensemble of ECG leads as a set of independent random variables. The best linear minimum-variance unbiased estimator of the complexity descriptor will thus be given by the weighted mean of Eq. (7) [36]. As a result, greater weight is given to values coming from lower-variance distributions. The flow chart resuming the main processing stages of our method is represented in Fig. 2.

### 2.7. Choice of NMSE characteristic parameters

Some considerations about the tuning of NMSE characteristic parameters should be mentioned, i.e., the number $S$ of AA segments which need to be processed, besides the number of spatial topographies $n$ used for AA signal estimation. Concerning the value of $S$, experimental evidence in [29] shows that in most patients NMSE decreases and remains constant after a certain threshold $S$ value. Since the error variation flattens from $S \approx 4$ segments, we set this value prior to signal decomposition. This choice is also supported in the present study by the evolution of $\widetilde{\mu}_{\mathrm{WPCA}_8}$ as a function of the number of segments $S$, assuming that their size is fixed and equal to $N_S$ and taking into account constraints derived from the ECG recording length available in our database. As Fig. 3 shows, the index keeps quite a constant value when $S$ increases. In addition, even when segment length $N_S$ changes, parameter variations are quite limited (below 10%), as shown in Fig. 4. This result confirms the robustness of the predictor put forward to the choice of tuning

Please cite this article in press as: M. Meo, et al., Catheter ablation outcome prediction in persistent atrial fibrillation using weighted principal component analysis, Biomed. Signal Process. Control (2013), http://dx.doi.org/10.1016/j.bspc.2013.02.002

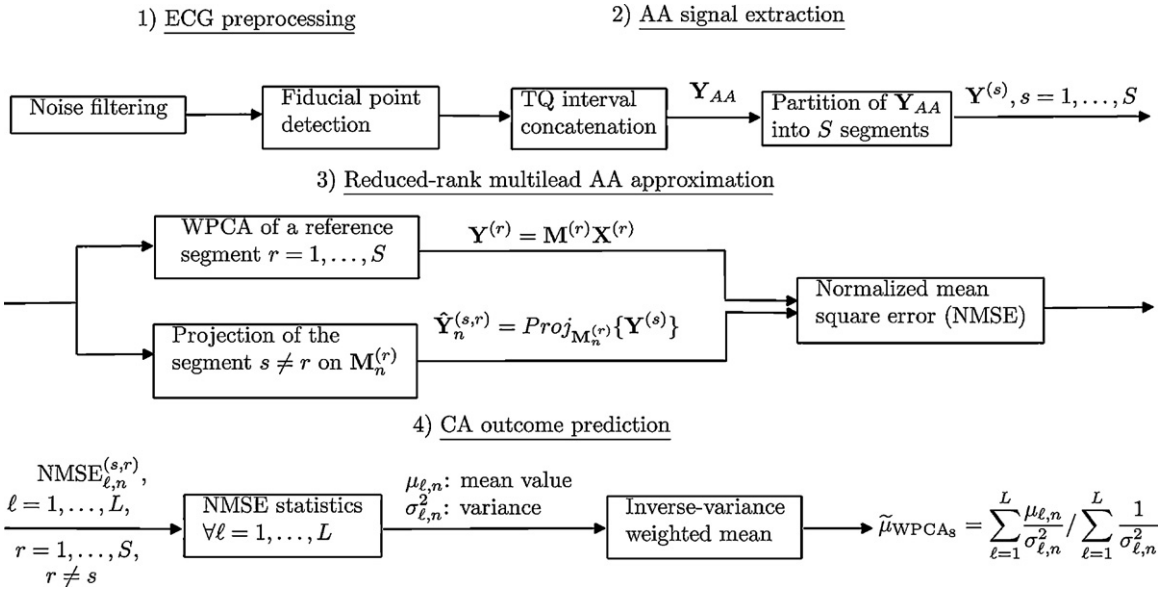


**Fig. 2.** Flow chart of the algorithm yielding the proposed CA outcome predictor $\widetilde{\mu}_{\mathrm{WPCA}_8}$.

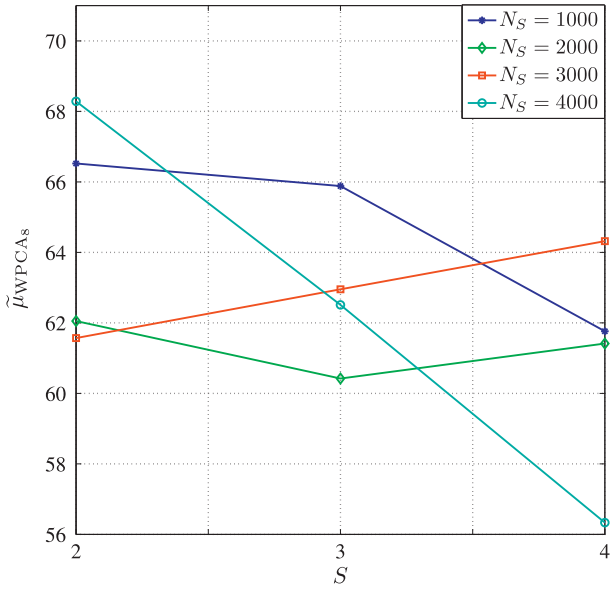


**Fig. 3.** Evolution of $\widetilde{\mu}_{\mathrm{WPCA}_8}$ as a function of the number of segments $S$.

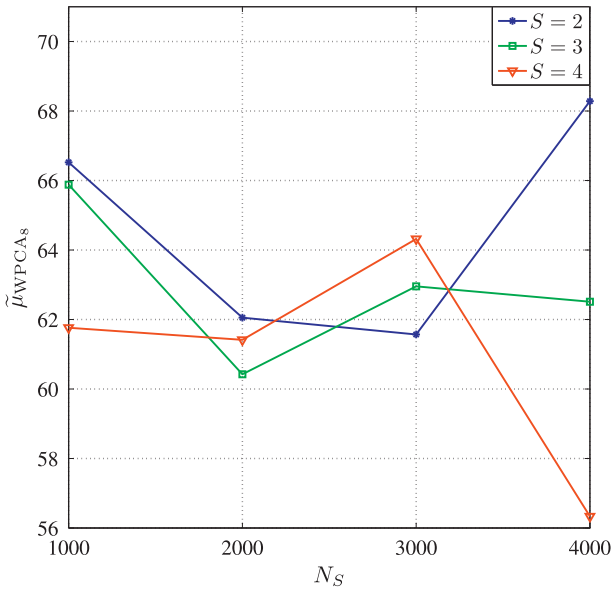


**Fig. 4.** Evolution of $\widetilde{\mu}_{\mathrm{WPCA}_8}$ as a function of the number of samples per segment $N_S$.

parameters and supports our choice of setting a unique value for $S$ for all patients in order to simplify the algorithm.

Concerning estimation performance, as WPCA rationale assumes that the first PC retains the most of the AA global variance, the rank-1 approximation of AA observations by projecting them over the dominant PC is computed. Indeed, such a reconstruction allows not only underlining the most descriptive components in terms of variance, but also suppressing irrelevant and/or noisy elements that can deteriorate signal content. Further experimental results are presented later in the paper (Section 3) and support the choice of setting $n = 1$, so the corresponding subscript will be omitted in the sequel for convenience. Finally, as WPCA is an iterative algorithm (described in the Appendix), a stopping criterion has been introduced, based on a convergence tolerance $\epsilon = 10^{-5}$ defined before Eq. (9). In order to assess WPCA computational

**Table 1**
Assessment of WPCA convergence characteristics: average number of iterations for convergence $\epsilon = 10^{-5}$.

| $N_S$ | $s$ | | | |
|---|---|---|---|---|
| | 1 | 2 | 3 | 4 |
| 1000 | 96 | 84 | 114 | 93 |
| 2000 | 92 | 100 | 92 | 96 |
| 3000 | 84 | 90 | 92 | 103 |
| 4000 | 85 | 98 | 101 | 112 |

**Table 2**
Assessment of WPCA convergence characteristics: average final value of WLS convergence criterion $C^*$ (Eq. (9)) after convergence, with $\epsilon = 10^{-5}$) [n.u.]. Values normalized by a scaling factor equal to $10^{-6}$.

| $N_S$ | $s$ | | | |
|---|---|---|---|---|
| | 1 | 2 | 3 | 4 |
| 1000 | 9.0 | 8.8 | 9.1 | 8.9 |
| 2000 | 8.8 | 9.0 | 8.6 | 9.2 |
| 3000 | 8.6 | 9.1 | 9.1 | 8.7 |
| 4000 | 9.0 | 8.9 | 8.9 | 9.0 |

Please cite this article in press as: M. Meo, et al., Catheter ablation outcome prediction in persistent atrial fibrillation using weighted principal component analysis, Biomed. Signal Process. Control (2013), http://dx.doi.org/10.1016/j.bspc.2013.02.002

**Table 3**
Interpatient statistical analysis and CA outcome prediction performance (n.u.: normalized units).

| | Successful CA | Failing CA | $p$-Value | AUC | Best cut-off |
|---|---|---|---|---|---|
| $\widetilde{\mu}_{WPCA_8}$ [n.u.] | $70.76 \pm 17.74$ | $37.54 \pm 20.01$ | 0.0013 | 0.91 | 40.64 |
| $\widetilde{\mu}_{WPCA_{12}}$ [n.u.] | $63.03 \pm 18.12$ | $61.64 \pm 20.87$ | 0.88 | 0.47 | 53.76 |
| $\widetilde{\mu}_{PCA_8}$ [n.u.] | $65.68 \pm 19.27$ | $37.59 \pm 21.88$ | 0.0082 | 0.84 | 45.57 |
| $\widetilde{\mu}_{PCA_{12}}$ [n.u.] | $65.85 \pm 28.41$ | $44.09 \pm 27.49$ | 0.12 | 0.76 | 45.57 |
| $NMSE_{WPCA_8}$ [n.u.] | $54.24 \pm 25.89$ | $50.24 \pm 23.04$ | 0.74 | 0.57 | 45.64 |
| $NMSE_{WPCA_{12}}$ [n.u.] | $85.67 \pm 14.62$ | $86.78 \pm 17.41$ | 0.75 | 0.54 | 95.32 |
| $NMSE_{PCA_8}$ [n.u.] | $45.56 \pm 26.93$ | $30.35 \pm 26.93$ | 0.19 | 0.64 | 49.03 |
| $NMSE_{PCA_{12}}$ [n.u.] | $67.80 \pm 22.11$ | $80.73 \pm 14.48$ | 0.18 | 0.69 | 69.00 |
| $D(V_1)$ [mV] | $0.08 \pm 0.03$ | $0.06 \pm 0.01$ | 0.03 | 0.80 | 0.05 |
| $SampEn(L_s, r_s^{(A)})$ [n.u.] | $2.82 \pm 0.39$ | $3.06 \pm 0.43$ | 0.21 | 0.70 | 3.12 |
| $SampEn(L_s, r_s^{(B)})$ [n.u.] | $2.42 \pm 0.38$ | $2.66 \pm 0.43$ | 0.20 | 0.70 | 2.73 |
| $SampEn(L_s, r_s^{(C)})$ [n.u.] | $2.14 \pm 0.37$ | $2.39 \pm 0.42$ | 0.20 | 0.70 | 2.44 |
| $AFCL_{V_1}$ [ms] | $139.63 \pm 19.66$ | $121.75 \pm 23.83$ | 0.09 | 0.71 | 129.87 |

load, the number of iterations for convergence and the final value of WLS convergence criterion $C^*$ (introduced in Eq. (9) in the Appendix) are computed for a fixed $N_S$ value. These values are first computed on each segment $s = 1, \ldots, 4$ and then averaged over the 20-patient database. Test results are reported in Tables 1 and 2. We can remark that both parameter values do not significantly change when passing from a segment to the following one, and that computational burden is relatively low in terms of iterations. A similar result is obtained when considering variations in the number of samples per segment $N_S$. This further evidence supports the robustness of our method to the choice of tuning parameters, as the algorithm converges to satisfactory results in all cases.

### 2.8. Statistical analysis and classification performance assessment

As displayed in Table 3, categories under examination are referred to as "Successful CA" and "Failing CA". All parameters are expressed as mean ± standard deviation. First, Lilliefors' test was run to verify data normality. Differences between successful and failing CA procedures were statistically determined by an unpaired Student's $t$-test if data were sampled from a Gaussian distribution, a Wilcoxon rank sum test otherwise. The $p$-values output by each unpaired test are obtained under a confidence level $\alpha = 0.05$, and they are reported in Table 3 as well. Binary classification accuracy of each feature is quantified by the area under its receiver operator curve (ROC), or area under curve (AUC), whose value is correlated with the maximization of sensitivity and specificity, i.e., the true positive and true negative rates, respectively.

## 3. Results

Our 8-lead descriptor $\widetilde{\mu}_{WPCA_8}$ is compared with its 12-lead counterpart $\widetilde{\mu}_{WPCA_{12}}$. Moreover, the final weighted mean of NMSE values has also been computed for each lead subset after performing a rank-1 approximation by classical PCA, thus obtaining $\widetilde{\mu}_{PCA_8}$ and $\widetilde{\mu}_{PCA_{12}}$, respectively. A comparison between multilead descriptors and conventional single-lead methods is drawn as well. Accordingly, AA amplitude $D(V_1)$ is computed on lead $V_1$ according to the algorithm proposed in [37,38]. Moreover, atrial fibrillation cycle length (AFCL), widely known as a predictor of AF termination by CA, is also determined on the same electrode. Its measure is manually determined as described in [39]. More specifically, its value is obtained by averaging temporal distance between 30 consecutive f-waves, thus giving $AFCL_{V_1}$ as output. In addition, we examine a single-lead complexity measure based on the NMSE value computed on $V_1$ either by applying WPCA or classical PCA. Such decompositions are accomplished both on the full ensemble of ECG leads and the reduced 8-lead subset, thus resulting in $NMSE_{WPCA_8}$, $NMSE_{WPCA_{12}}$, $NMSE_{PCA_8}$ and $NMSE_{PCA_{12}}$, respectively, as outputs. A parallel with a non-linear complexity descriptor, the sample entropy SampEn [24,26,40], has been drawn as well on $V_1$. Two parameters have to be tuned prior to its computation: $L_s$ and $r_s$. Parameter $L_s$ is defined as the length of the sequences the ECG recording is split into. Such segments are then compared, and the tolerance for accepting matches is assessed by the threshold $r_s$. This parameter is chosen as a fraction of the AA input signal standard deviation on $V_1$, denoted $\sigma_{V_1}$, so as to assure the translation and scale invariance of SampEn. Parameter values have been tuned according to the guidelines given in [24], so we set $L_s = 2$ besides three values of $r_s$, namely, $r_s^{(A)} = 0.1\sigma_{V_1}$, $r_s^{(B)} = 0.15\sigma_{V_1}$ and $r_s^{(C)} = 0.2\sigma_{V_1}$.

The generalization power of our analysis to an independent dataset is validated by means of a leave-one-out cross-validation technique. More precisely, AUC values have been computed on every possible subset of 19 patients, and then averaged over the 20 subsets. AUC values describing the classification power of each descriptor are shown in Table 3, besides the corresponding optimal cut-off points, providing both the highest sensitivity and the highest specificity on the whole 20-patient database. Fig. 5 plots the

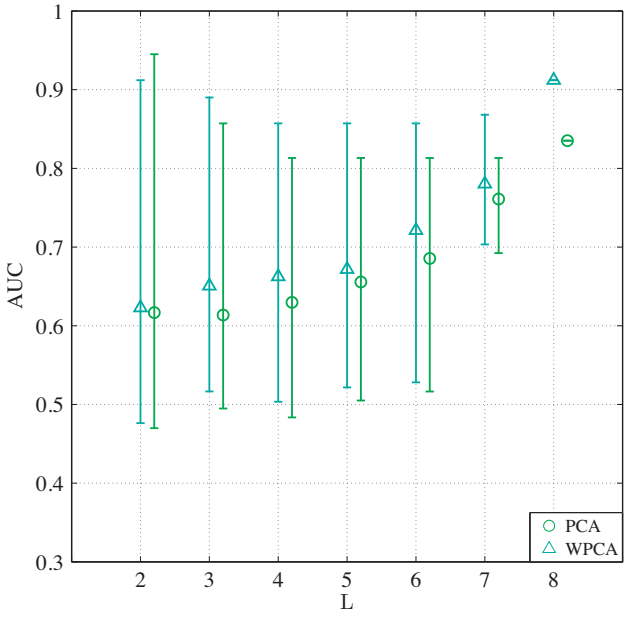


**Fig. 5.** AUC values characterizing $\widetilde{\mu}_{WPCA_L}$ prediction performance as a function of the size $L$ of the subset of the 8 independent ECG leads ($S = 4$, $n = 1$). WPCA: rank-1 decomposition of the atrial signal in the ECG lead subsets according to the WPCA approach; PCA: rank-1 decomposition of the atrial signal in the ECG lead subsets according to the PCA approach.

Please cite this article in press as: M. Meo, et al., Catheter ablation outcome prediction in persistent atrial fibrillation using weighted principal component analysis, Biomed. Signal Process. Control (2013), http://dx.doi.org/10.1016/j.bspc.2013.02.002

**Table 4**
ECG lead subsets with optimal prediction performance of $\widetilde{\mu}_{WPCA_8}$.

| Number of leads ($L$) | Leads |
|---|---|
| 2 | I, $V_1$ |
| 3 | I, II, $V_2$ |
| 4 | I, $V_2$, $V_3$, $V_5$ |
| 5 | [I, II, $V_2$, $V_4$, $V_5$] |
| | [I, II, $V_1$, $V_3$, $V_6$] |
| 6 | I, II, $V_2$, $V_3$, $V_4$, $V_6$ |
| 7 | I, II, $V_1$, $V_2$, $V_3$, $V_4$, $V_5$ |

AUC values describing the classification performance of $\widetilde{\mu}_{WPCA_L}$ as a function of the number $L$ of leads retained in the analysis. For each value of $L$ ranging from 2 up to 8, $\widetilde{\mu}_{PCA_L}$ value has been computed for all $8!/((8-L)!\,L!)$ possible ensembles of leads. For each lead combination, CA outcome prediction performance has been assessed from the corresponding values of $\widetilde{\mu}_{WPCA_L}$, and validated by the leave-one-out technique. For each size $L$, the minimum, maximum and mean AUC values over all $L$-lead subsets were obtained as a function of the subset dimension $L$, and their related ranges of values are displayed in Fig. 5. The lead combinations with the best prediction performance for each subset dimension are shown in Table 4. The application of PCA on a single lead ($L=1$) has been excluded from this test, since in this case the method is equivalent to single-lead analysis.

In our application, we deal with multivariate decomposition techniques based on the maximization of the variance of the AA signal, conveying information about AF spatio-temporal distribution. Hence, another crucial point of our investigation is the effect of such techniques on AA signal energy content. More specifically, the input AA signal variance has been determined on each ECG lead, yielding the atrial power distribution represented by the vector $\boldsymbol{\sigma}^2_{AA} = [\sigma_{AA_1}^2, \sigma_{AA_2}^2, \ldots, \sigma_{AA_L}^2]^T$, with $L=8$. Effects of the multilead weighting scheme on the decompositions of the observed AA signal are also compared to those obtained by standard PCA. The rank-1 approximations $\mathbf{Y}$ computed by WPCA and PCA yield atrial power distribution vectors $\boldsymbol{\sigma}^2_{WPCA}$ and $\boldsymbol{\sigma}^2_{PCA}$, respectively. These parameters have been computed over the whole persistent AF database and averaged over all patients; their spatial distribution is plotted in Fig. 6. This figure evaluates the energy content of data reconstructions computed by each decomposition, as well as their capability of effectively approximating the original signal. Following this line, this evaluation has been accomplished in the framework of CA outcome prediction as well. In particular, we tested whether AA signal energy $\sigma^2_{AA}$ associated with each lead can effectively perform as a predictor of the ablation result; hence, the quantification of their classification accuracy on each ECG lead by means of the AUC criterion, whose values are displayed in Fig. 7. The same analysis is led on the energy values computed on the rank-1 approximations output by PCA and WPCA, $\sigma^2_{PCA}$ and $\sigma^2_{WPCA}$, respectively, also plotted in Fig. 7. Finally, further tests confirm the validity of the model introduced in Eq. (5) by assessing CA outcome prediction performance on the basis of different definitions of the weight matrix $\mathbf{W}^{(r)}$ as will be discussed in Section 4.5.

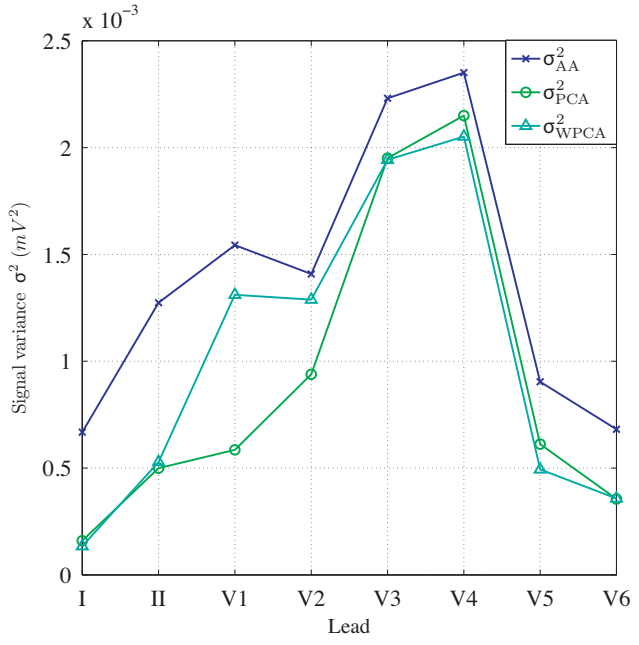


**Fig. 6.** Effects of the multilead weighting scheme on AA reconstruction. $\sigma^2_{AA}$: variance of the input AA signal per lead; $\sigma^2_{PCA}$: variance per lead of the rank-1 AA signal approximation by PCA; $\sigma^2_{WPCA}$: variance per lead of the rank-1 AA signal approximation by WPCA.

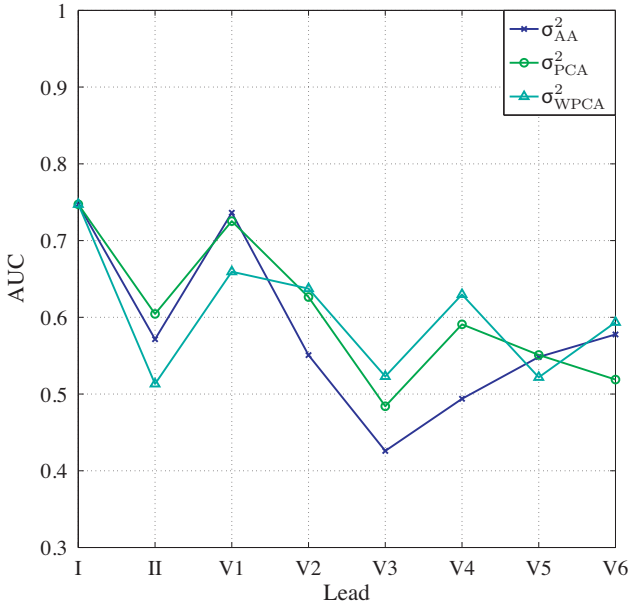


**Fig. 7.** Assessment of CA outcome prediction performance of single-lead energy descriptors. $\sigma^2_{AA}$: energy of the input AA signal per lead; $\sigma^2_{PCA}$: energy per lead of the rank-1 AA signal approximation by PCA; $\sigma^2_{WPCA}$: energy per lead of the rank-1 AA signal approximation by WPCA.

## 4. Discussion

This work investigates noninvasive measures of AA spatio-temporal variability and their link to CA outcome prediction in persistent AF. The main results can be summarized as follows. Firstly, spatial variability of the standard ECG proves to be a useful tool to describe AF content and offer a wider perspective about the evolution of the disease during CA, thus helping its outcome prediction. In the second place, an index conventionally employed as a classifier of AF organization type is herein characterized so as to assess CA effect. Information about AA signal coming from multiple ECG leads is exploited by applying WPCA, which efficiently compresses AF content in a unique, significant PC, thereby minimizing the impact of polluting signal components. The weights used in WPCA seem to automatically enhance the role of the most descriptive ECG leads, unlike PCA, which equally weights all ECG leads. This filtering action is also performed by selecting the 8-lead ensemble introduced in Section 2.2, so suppressing linear dependencies between certain leads due to their spatial location. These aspects are discussed in more detail in the sequel.

Please cite this article in press as: M. Meo, et al., Catheter ablation outcome prediction in persistent atrial fibrillation using weighted principal component analysis, Biomed. Signal Process. Control (2013), http://dx.doi.org/10.1016/j.bspc.2013.02.002

### 4.1. CA outcome prediction in the WPCA multilead framework

Our experimental results point out the advantages of the multilead strategy which considerably outperforms conventional predictors computed in only one ECG lead. Concerning single-lead AF complexity measures determined by PCA on different sets of ECG leads, i.e., $NMSE_{PCA_8}$ and $NMSE_{PCA_{12}}$, not only statistically significant interpatient differences cannot be observed, but AUC values related to their discrimination capability are also extremely low. Similar conclusions can be drawn when examining the equivalent parameters obtained in $V_1$ when approximating data by means of WPCA ($NMSE_{WPCA_8}$, $NMSE_{WPCA_{12}}$). These results could be explained by the limited outlook of single-lead complexity measures, which ignore interlead relationships. Relevant information from other electrodes is neglected, thus reducing discrimination capabilities. Furthermore, as lead $V_1$ is close to the right atrial free wall, there is the risk of neglecting useful information about other important anatomical areas, such as the left atrium (LA) and the PVs, which play a crucial role in AF initiation and maintenance [41]. In [42], it is shown that $V_1$ is the lead that best explains left atrial activity in two subjects affected by atrial tachycardia confined to the LA. However, AF mechanisms are generally more complex, and our results in Section 4.5 indicate in any case that, concerning CA outcome prediction, lead $V_1$ does not depict important information about ablation effects that could be present in other leads. Also, concerning nonlinear AF complexity indices such as sample entropy, no statistically significant interclass differences can be remarked, regardless of the values of tuning parameters. Not only sample entropy index is affected by the same shortcomings typical of the other single-lead features, but it is also necessary to set values of its tuning parameters prior to its computation.

By contrast, by means of WPCA, ECG spatial diversity highlights statistically significant differences between the categories examined. As displayed in Table 3, higher values of the multilead descriptor $\widetilde{\mu}_{WPCA_8}$ are significantly correlated with CA success. As its mathematical definition in Eq. (7) shows, the NMSE inter-segment variance provides a quantitative criterion for the assessment of the spatio-temporal variability of the AA signal: leads exhibiting more stable and repetitive patterns give a more relevant contribution to the weighted mean $\widetilde{\mu}_{WPCA_8}$, so they have stronger influence. The inter-segment variance acts as a lead selector: it enhances ECG electrodes where not only the signal shows the most stable waveform, but it is also likely to yield a more accurate signal estimation, with a lower degree of uncertainty.

### 4.2. A comparison with standard clinical predictors of CA outcome

In the first place, selection of patients to be treated by CA is guided by considerations about some clinical data, such as LA diameter and AF duration. Indeed, it is widely known that when the LA is markedly dilated CA is less likely to be effective, as a larger LA is linked to a more advanced degree of the pathology. Similar remarks can be made about AF duration, correlated with its chronification level [14]. In [43] it is demonstrated that CA outcome prediction in paroxysmal AF is notably improved by the knowledge about some features, primarily the presence of non-PV drivers and dominant frequencies both in right and left atrium. Nevertheless, the most of these parameters are invasively acquired and known only at the moment of the procedure. This motivates the interest in predictive features that can be extracted without risk to the patient in a cost-efficient manner, as those derived from the ECG.

Analysis of the AA amplitude as rendered by $D(V_1)$ arouses different remarks. Actually, we can notice the satisfactory ability to distinguish between successful and failing ablations, as well as the effective reproduction of results manually reported in previous works using a different persistent AF database [8]. Such a descriptor can effectively capture AA signal amplitude characteristics if the pattern is sufficiently regular and f-waves are easily detectable, although interpolation operations can be hampered by residual spurious peaks or too irregular patterns. What is more, no information about AF spatio-temporal repetitiveness is provided by this feature.

The study presented in [39] assesses the predictive role of AFCL measured on surface ECG for CA of persistent AF. However, as its value is manually acquired, there is a lack of reproducibility and prediction reliability. Moreover, experimental results show that such parameter, defined as $AFCL_{V_1}$, does not underline statistically significant differences between the categories under examination using lead $V_1$. Furthermore, as it is usually determined in only one electrode, it is affected by the shortcomings typical of single-lead predictors. In addition, correlation between ECG-based parameters and intracardial measures has not been confirmed in some studies [44].

### 4.3. Weighted and standard PCA: a comparison

Even though standard PCA is capable of discriminating between successful and failing CA procedures as well, results concerning $\widetilde{\mu}_{WPCA_8}$ show that classification quality can be further improved by our a priori knowledge about atrial observations in the form of the weights used in WPCA. On further analysis, AA standard deviation measured on each ECG electrode proves to be a reliable index, since it does not only weight AF temporal dispersion, but it is also a statistical measure of uncertainty. Indeed, if AA patterns on certain leads are excessively irregular and/or variable, the corresponding inverse standard deviation values automatically reduce their influence. This selective action seems to boost the compression power of the decomposition. More specifically, the effect of possible redundancies is already reduced before computing the iterative minimization algorithm by selecting the 8 linearly independent ECG leads, so that the most discriminant AA components are put into evidence more easily. In Fig. 5 the AUC criterion quantifies the classification performance of $\widetilde{\mu}_{WPCA_L}$ and $\widetilde{\mu}_{PCA_L}$ as a function of the number of ECG leads exploited for the prediction selected among the 8 independent leads. Classification results obtained using WPCA outperform those by PCA, especially as size $L$ increases. This figure also confirms the benefits derived from the spatial variability of the standard ECG. The higher the number of leads employed, the more accurate CA result prediction, assessed by higher mean AUC values.

Further advantages derived from the weighting framework are displayed in Fig. 6. First of all, it can be noticed that the trend of $\sigma^2_{WPCA}$ values is very similar to that of $\sigma^2_{AA}$. In addition, $\sigma^2_{WPCA}$ values are closer to $\sigma^2_{AA}$ than those obtained when performing classical PCA ($\sigma^2_{PCA}$), thereby quantifying a lower error of reconstruction of the original data. Energy values obtained after AA signal approximation, either by PCA or WPCA, are lower than those computed directly on input data because of the low-rank representation effect. It can be inferred that WPCA can better preserve energy content of the AA signal and condense it more efficiently in a single, maximum-variance PC than conventional PCA. Differences between these decompositions in terms of the amount of information retained by the rank-1 approximation are particularly evident in $V_1$ and $V_2$, which represent the reference leads for AF analysis in medical practice, owing to their proximity to the right atrium. Note how WPCA significantly enhances, in an automated fashion, the relevance of these leads in the AA signal decomposition. The use of these energy-descriptors in single-lead prediction does not provide satisfactory results, as shown in Fig. 7. Indeed, their prediction performance is poor, and also highly dependent on

Please cite this article in press as: M. Meo, et al., Catheter ablation outcome prediction in persistent atrial fibrillation using weighted principal component analysis, Biomed. Signal Process. Control (2013), http://dx.doi.org/10.1016/j.bspc.2013.02.002

the lead considered. In general, these results confirm the need for an adequate combination of atrial signal contributions from different ECG leads in a more robust multilead framework, capable of filtering out uninformative AA signal features and exploiting ECG spatial variability. However, the importance of their contribution is significantly reduced when applying PCA, thus losing relevant information about AF energy content in the associated heart sites. Conversely, the WPCA scheme can effectively improve CA outcome prediction by reinforcing the most discriminative features of input data thanks to the prior knowledge about AA signal energy distribution.

### 4.4. Alternative definitions of the weight matrix

The choice of the inverse standard deviation values as $\mathbf{W}^{(r)}$ weights confirms our hypothesis about AA signal representation illustrated in Section 2.5. Conversely, other weighting schemes are not able to give comparable classification results. For example, the weight matrix depending on AA standard deviation values per lead $\mathbf{W}^{(r)} = [\sigma_1^{(r)}, \sigma_2^{(r)}, \ldots, \sigma_L^{(r)}]^T\mathbf{1}$ does not manage to properly emphasize ECG lead contributions, thus showing a weak predictive power (AUC = 0.53, $p$-value = 0.98). These results seem to corroborate our AF model, as AA maximum-power components seem unable to selectively enhance the most informative contributions by means of the weighting structure.

In further experiments, alternative weight matrices $\mathbf{W}^{(r)}$ have also been tested. For instance, one of the attempted strategies consists in giving more weight to leads better explained by a reduced-rank PCA approximation, thus defining $\mathbf{W}^{(r)}$ elements as a function of the inverse value of standard deviation of the error between original data and rank-1 PCA approximation per lead ($\mathbf{W}^{(r)} = [(\sigma_{1_N}^{(r)})^{-1}, (\sigma_{2_N}^{(r)})^{-1}, \ldots, (\sigma_{L_N}^{(r)})^{-1}]^T\mathbf{1}$). However, no significant differences between effective and failing CA procedures have been found in this case (AUC = 0.67, $p$-value = 0.69). In other tests, we hypothesize that $\mathbf{W}^{(r)}$ components depend on the value of the standard deviation itself ($\mathbf{W}^{(r)} = [\sigma_{1_N}^{(r)}, \sigma_{2_N}^{(r)}, \ldots, \sigma_{L_N}^{(r)}]^T\mathbf{1}$), although similar poor results are obtained (AUC = 0.63, $p$-value = 0.37). This leads us to conclude that focusing on noisy components that may be present in the AA signal does not actually improve the selective action of the weighting scheme, whereas considering variance of the whole signal gives more emphasis to its most informative components, thus improving prediction accuracy.

### 4.5. ECG-lead selection

Classification performance of multilead CA predictors proves to be more accurate when reduced-rank approximations are computed on the subset of 8 independent leads rather than the whole standard ECG. This result is in line with recent previous works [38]. In clinical centers, all leads of the standard ECG are analyzed so that projections of the resultant vectors in 2 orthogonal planes at different angles can be compared, so improving pattern recognition [18]. However, WPCA computation over the subset of 8 independent leads defined above seems to increase the efficacy of its filtering action, as part of redundant information is already suppressed before the decomposition, and the model captures the natural variation underlying the data more easily. These considerations justify the fact that descriptors extracted from the whole ECG, namely, $\widetilde{\mu}_{\mathrm{WPCA}_{12}}$ and $\widetilde{\mu}_{\mathrm{PCA}_{12}}$, are outperformed by their 8-lead counterparts.

Table 4 displays the groups of leads which best help discriminating between successful and failing procedures, and give the most relevant contribution to the computation of the weighted mean $\widetilde{\mu}_{\mathrm{WPCA}_8}$ in the prediction scenario. Some considerations can be made about the role of certain leads in CA outcome prediction. In particular, we can remark that lead $V_1$ does not provide the main contribution to CA outcome prediction. In fact, other leads, such as I, II, $V_2$, recur more frequently. This evidence is in contrast with standard medical practice, and it can be probably explained by the placement of lead $V_1$, not close enough to critical sites responsible for AF genesis and maintenance such as the PVs and the LA, commonly acknowledged as potential AF sources. This seems to be confirmed by the recurrence of at least one lead close to the left side of the heart in each $L$-size subset, for instance, $V_5$ and $V_6$. We can conclude that the presence of leads representing heart electrical activity on multiple planes supports the hypothesis that clinical information coming from multiple electrode locations can improve ablation outcome prediction as compared to classical single-lead approaches, as discussed in Section 4.1.

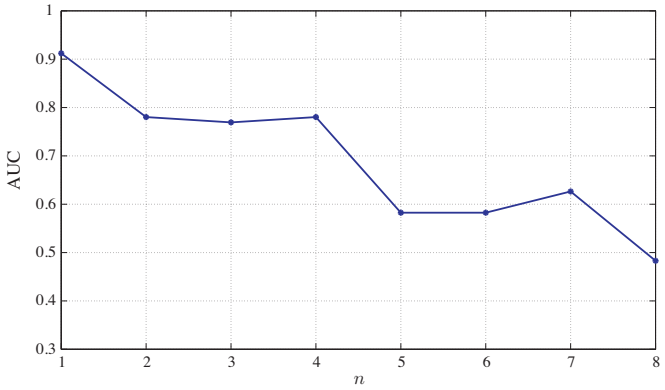


**Fig. 8.** AUC values describing $\widetilde{\mu}_{\mathrm{WPCA}_8}$ prediction performance as a function of the rank $n$ of the WPCA decomposition.

### 4.6. Benefits of reduced-rank WPCA approximations to the AA signal

Fig. 8 illustrates the advantages provided by data compression carried out by WPCA, and seems to justify the choice of rank-1 approximations ($n = 1$) made in Section 2.7. Indeed, AUC values related to our multilead predictor $\widetilde{\mu}_{\mathrm{WPCA}_8}$ have been computed by varying the number of PCs $n$ retained in the WPCA truncation in Eq. (2), which ranges from 1 (the value set for our algorithm) to 8 (full-rank decomposition). The quality of CA outcome prediction considerably worsens when increasing the truncation rank, and $\widetilde{\mu}_{\mathrm{WPCA}_8}$ exhibits weak discriminating capabilities when assuming more than 4 PCs. The fewer PCs employed in the decomposition, the better the classification performance, as if the dominant PCs preserved the discriminative power of the complexity index. Indeed, noisy and/or redundant elements are typically ascribed to the very last PCs, while preserving the most representative features of the AA signal in the dominant ones. A similar benefit of rank reduction was obtained in [38] in the context of short-term CA outcome prediction based on amplitude parameters computed from low-rank PCA approximation.

### 4.7. Links with AF spatio-temporal complexity

As our research demonstrates, CA outcome prediction based on WCPA of multilead ECG signals proves to be effective. However, the proper link between the NMSE-based predictor proposed and AF spatio-temporal complexity cannot be established in the present work for lack of simultaneous invasive recordings. Such a connection can only be suggested by the results presented in [11], which showed the correlation between the NMSE measure in $V_1$ and AF organization. Accordingly, the potential relation

Please cite this article in press as: M. Meo, et al., Catheter ablation outcome prediction in persistent atrial fibrillation using weighted principal component analysis, Biomed. Signal Process. Control (2013), http://dx.doi.org/10.1016/j.bspc.2013.02.002

between CA outcome and AF organization by means of our multilead characterization of the NMSE index should be further investigated.

### 4.8. Limitations of the study

This research is hampered by the limited size of our persistent AF database, making it difficult to generalize the results obtained. No comparison with invasive recordings is developed in our study, so possible relations with endocardial electrical phenomena depicting AF spatio-temporal complexity cannot be analyzed. Moreover, the short follow-up length established for some patients can increase error probability when assessing ablation success. Finally, further attention should be paid to the implementation modalities of the WPCA weight matrix **W**. Roughly speaking, even though the methodology illustrated in Section 2.5 and further discussed in Section 4.4 proves to be robust and appropriate for fulfilling long-term CA outcome prediction in the available database, alternative computational strategies could be conceived for a deeper comprehension of AF electrophysiology.

## 5. Conclusions

This work has examined the role of quantitative indices computed on the surface standard ECG in predicting CA outcome. These parameters are derived from the NMSE of reduced-rank PCA approximations to the AA signal, recently shown to quantify AF spatio-temporal organization. Even though we have not proved their ability to assess AF organization, our investigation has demonstrated that contributions from several ECG leads can be adequately combined so as to accomplish preprocedural long-term CA outcome prediction in persistent AF patients. Compared with conventional PCA, WPCA is able to better capture the spatial variability typical of multilead recordings by automatically enhancing the most significant contributions from an appropriate subset of ECG leads. The inspection of NMSE spatial distribution can offer a wider perspective of AF evolution on the heart substrate, thus overcoming the limited characterization typical of single-lead strategies. Moreover, our predictor is more robust to lead selection than single-lead approaches, so it can be particularly advantageous under particular circumstances, e.g., when electrodes get accidentally loose or disconnected from the patient's body. Another positive effect of WPCA concerns data compression into a single, maximum-variance PC, as the rank-1 approximation to the AA signal seems to retain its most essential features while rejecting unnecessary information. Our research has demonstrated that information capable of predicting CA outcome can be efficiently extracted from the multilead ECG by means of a robust approach based on a WPCA decomposition of the AA signal over a suitable ensemble of linearly independent ECG leads. Alternative multivariate decomposition techniques have to be examined, as well as further strategies to select weight matrix **W** in the WPCA framework.

## Acknowledgements

This work is partly supported by the French National Research Agency under contract ANR-2010-JCJC-0303-01 "PERSIST". Marianna Meo is funded by a doctoral grant from the French Ministry of Higher Education and Research. Her activity is also funded by a one-year grant awarded in 2012 by the DreamIT Foundation in partnership with the University of Nice Sophia Antipolis.

## Appendix. Algorithm for WPCA computation

WLS minimization is achieved by the following optimization algorithm proposed in [35]:

- Initialize $\mathbf{Y}_0$ and compute $h_0 = h(\mathbf{Y}_0|\mathbf{Y}, \mathbf{W})$, where $h(\cdot)$ is the WLS cost function given by Eq. (4).
- For $i = 0, 1, 2, \ldots$ until convergence
  1. Compute a gradient-descent iteration on the WLS cost, as $\widetilde{\mathbf{Y}}_i = \mathbf{Y}_i + \beta \mathbf{W} * \mathbf{W} * (\mathbf{Y} - \mathbf{Y}_i)$, where $\beta = w_M^{-2}$, $w_M$ is the maximum weight of **W**.
  2. Compute $\mathbf{Y}_{i+1}$ as the reduced-rank model fitting the data $\widetilde{\mathbf{Y}}_i$:
  $$\mathrm{Y}_{i+1} = \underset{\mathrm{Y}}{\mathrm{argmin}} \|\widetilde{\mathbf{Y}}_i - \mathrm{Y}\|_{\mathrm{F}}^2 \quad (8)$$
  subject to the orthogonality constraints on **Y**. This is given by the best rank-$r$ approximation (determined, e.g., via the SVD) of the matrix $\widetilde{\mathbf{Y}}_i$ obtained at the previous step.
  3. Compute $h_{i+1} = h(\mathbf{Y}_{i+1}|\mathbf{Y}, \mathbf{W})$. Given a fixed, small tolerance $\epsilon$, if $C^* < \epsilon$, where:
  $$C^* = (h_i - h_{i+1})/h_i, \quad (9)$$
  the convergence is reached; otherwise set $i = i + 1$ and repeat the algorithm from Step 1 until convergence.
- End

More specifically, the criterion is monotonically minimized according to Eq. (8), knowing that $\widetilde{\mathbf{Y}}$ depends on the multivariate input signal **Y**, the weight matrix **W** and the model **Y** at the current iteration.

Different procedures for initializing **Y** have been envisaged in earlier works. Our implementation assumes to assign the OLS solution obtained by the standard PCA, so that $\mathbf{Y}_0$ equals the best rank-$r$ approximation determined without assigning loads to preferential leads.

## References

[1] K. Konings, C. Kirchhof, J. Smeets, et al., High-density mapping of electrically induced atrial fibrillation in humans, Circulation 89 (1994) 1665–1680.
[2] G. Moe, On the multiple wavelet hypothesis of atrial fibrillation, Archives Internationales de Pharmacodynamie et de Therapie 140 (1962) 183–188.
[3] P. Jaïs, M. Haissaguerre, D. Shah, et al., A focal source of atrial fibrillation treated by discrete radiofrequency ablation, Circulation 95 (1997) 572–576.
[4] A. Verma, A. Natale, Should atrial fibrillation ablation be considered first-line therapy for some patients? Why atrial fibrillation ablation should be considered first-line therapy for some patients, Circulation 112 (2005) 1214–1222.
[5] K. Nademanee, J. McKenzie, E. Kosar, et al., A new approach for catheter ablation of atrial fibrillation: mapping of the electrophysiologic substrate, Journal of the American College of Cardiology 43 (2004) 2044–2053.
[6] M. O'Neill, P. Jaïs, M. Hocini, et al., Catheter ablation for atrial fibrillation, Circulation 116 (2007) 1515–1523.
[7] H. Oral, A. Chugh, E. Good, Radiofrequency catheter ablation of chronic atrial fibrillation guided by complex electrograms, Circulation 115 (20) (2007) 2606–2612.
[8] I. Nault, N. Lellouche, S. Matsuo, et al., Clinical value of fibrillatory wave amplitude on surface ECG in patients with persistent atrial fibrillation, Journal of Interventional Cardiac Electrophysiology 26 (1) (2009) 11–19.
[9] A. Bollmann, D. Husser, L. Mainardi, et al., Analysis of surface electrocardiograms in atrial fibrillation: techniques, research, and clinical applications, Europace 8 (11) (2006) 911–926.
[10] M. Haïssaguerre, P. Sanders, M. Hocini, et al., Catheter ablation of long-lasting persistent atrial fibrillation: critical structures for termination, Journal of Cardiovascular Electrophysiology 16 (11) (2005) 1125–1137.
[11] P. Bonizzi, M.S. Guillem, A.M. Climent, J. Millet, V. Zarzoso, F. Castells, O. Meste, Noninvasive assessment of the complexity and stationarity of the atrial wavefront patterns during atrial fibrillation, IEEE Transactions on Biomedical Engineering 57 (9) (2010) 2147–2157.
[12] S. Petrutiu, N. Jason, G. Nijm, et al., Atrial fibrillation and waveform characterization, IEEE Engineering in Medicine and Biology Magazine 25 (6) (2006) 24–30.
[13] P. Bonizzi, O. Meste, V. Zarzoso, D.G. Latcu, I. Popescu, P. Ricard, N. Saoudi, Atrial fibrillation disorganization is reduced by catheter ablation: a standard ECG study, in: Proc. IEEE EMBC, 2010, pp. 5286–5289.

Please cite this article in press as: M. Meo, et al., Catheter ablation outcome prediction in persistent atrial fibrillation using weighted principal component analysis, Biomed. Signal Process. Control (2013), http://dx.doi.org/10.1016/j.bspc.2013.02.002

[14] H. Calkins, J. Brugada, D.L. Packer, et al., HRS/EHRA/ECAS expert consensus statement on catheter and surgical ablation of atrial fibrillation: recommendations for personnel, policy, procedures and follow-up, Heart Rhythm 4 (6) (2007) 816–861.
[15] C. Elayi, L. Di Biase, C. Barrett, et al., Atrial fibrillation termination as a procedural endpoint during ablation in long-standing persistent atrial fibrillation, Heart Rhythm 7 (2010) 1216–1223.
[16] J. Pan, W.J. Tompkins, A real-time QRS detection algorithm, IEEE Transactions on Biomedical Engineering 3 (3) (1985) 230–236.
[17] A. Cabasson, O. Meste, Time delay estimation: a new insight into the Woody's method, IEEE Signal Processing Letters 15 (2008) 573–576.
[18] J. Malmivuo, R. Plonsey, Bioelectromagnetism – Principles and Applications of Bioelectric and Biomagnetic Fields, Oxford University Press, New York, 1995.
[19] G.W. Botteron, J.M. Smith, A technique for measurement of the extent of spatial organization of atrial activation during atrial fibrillation in the intact human heart, IEEE Transactions on Biomedical Engineering 42 (6) (1995) 579–586.
[20] L. Faes, G. Nollo, M. Kirchner, E. Olivetti, F. Gaita, R. Riccardi, R. Antolini, Principal component analysis and cluster analysis for measuring the local organisation of human atrial fibrillation, Medical & Biological Engineering & Computing 39 (6) (2006) 636–656.
[21] G. Nollo, M. Marconcini, L. Faes, F. Bovolo, F. Ravelli, L. Bruzzone, An automatic system for the analysis and classification of human atrial fibrillation patterns from intracardiac electrograms, IEEE Transactions on Biomedical Engineering 55 (9) (2008) 2275–2285.
[22] L.T. Mainardi, A. Porta, G. Calcagnini, et al., Linear and nonlinear analysis of atrial signals and local activation period series during atrial fibrillation episodes, Medical and Biological Engineering and Computing 39 (2001) 249–254.
[23] G. Pagana, L. Galleani, S. Grossi, M. Ruo, E. Pastore, M. Poggio, G. Quaranta, Time-frequency analysis of the endocavitarian signal in paroxysmal atrial fibrillation, IEEE Transactions on Biomedical Engineering 59 (10) (2012) 2838–2844.
[24] J.S. Richman, J. Moorman, Physiological time-series analysis using approximate entropy and sample entropy, American Journal of Physiology: Heart and Circulatory Physiology 278 (2000) 2039–2049.
[25] R. Alcaraz, J.J. Rieta, A review on sample entropy applications for the non-invasive analysis of atrial fibrillation electrocardiograms, Biomedical Signal Processing 5 (1) (2010) 1–14.
[26] R. Alcaraz, J Hornero, J.J. Rieta, Enhancement of atrial fibrillation electrical cardioversion procedures through the arrhythmia organization estimation from the ECG, in: Proc. IEEE EMBC, 2010, pp. 122–125.
[27] L. Uldry, J. Van Zaen, Y. Prudat, L. Kappenberger, J.-M. Vesin, Measures of spatiotemporal organization differentiate persistent from long-standing atrial fibrillation, Europace 14 (8) (2012) 1125–1131.
[28] M.S. Guillem, A.M. Climent, F. Castells, et al., Noninvasive mapping of human atrial fibrillation, Journal of Cardiovascular Electrophysiology 5 (2009) 507–513.
[29] M. Meo, V. Zarzoso, O. Meste, D.G. Latcu, N. Saoudi, Catheter ablation outcome prediction in persistent atrial fibrillation based on spatio-temporal complexity measures of the surface ECG, in: Proc. Annual Int. Computing in Cardiology, vol. 38, Hagzhou, China, 2011, pp. 261–264.
[30] M. Meo, V. Zarzoso, O. Meste, D.G. Latcu, N. Saoudi, Nonnegative matrix factorization for noninvasive prediction of catheter ablation outcome in persistent atrial fibrillation, in: IEEE International Conference on Acoustics, Speech, and Signal Processing (ICASSP), Kyoto, Japan, 2012, pp. 601–604.
[31] F. Castells, P. Laguna, L. Sörnmo, et al., Principal component analysis in ECG signal processing, EURASIP Journal on Advances in Signal Processing 2007 (2006) 1–21.
[32] J. Rodríguez-Sotelo, E. Delgado-Trejos, D. Peluffo-Ordóñez, et al., Weighted-PCA for unsupervised classification of cardiac arrhythmias., in: Proc. IEEE EMBC, Buenos Aires, Argentina, 2010, pp. 1906–1909.
[33] J. Jansen, H. Hoefsloot, H.F.M. Boelens, et al., Analysis of longitudinal metabolomics data, Bioinformatics 20 (2004) 2438–2446.
[34] D. Skŏcaja, A. Leonardisa, H. Bischofb, Weighted and robust learning of subspace representations, Journal of Pattern Recognition 40 (2007) 1556–1569.
[35] A. Henk, L. Kiers, Weighted least squares fitting using ordinary least squares algorithms, Psycometrika 62 (2) (1997) 251–266.
[36] S. Kay, Fundamentals of Statistical Signal Processing: Estimation Theory, vol. I, Prentice Hall Signal Processing Series, 1993.
[37] M. Meo, V. Zarzoso, O. Meste, D.G. Latcu, N. Saoudi, Non-invasive prediction of catheter ablation outcome in persistent atrial fibrillation by exploiting the spatial diversity of surface ECG, in: Proc. IEEE EMBC, Boston, USA, 2011, pp. 5531–5534.
[38] M. Meo, V. Zarzoso, O. Meste, D.G. Latcu, N. Saoudi, Spatial variability of the 12-lead surface ECG as a tool for noninvasive prediction of catheter ablation outcome in persistent atrial fibrillation, IEEE Transactions on Biomedical Engineering 60 (1) (2013) 20–27.
[39] S. Matsuo, N. Lellouche, M.e.a. Wright, Clinical predictors of termination and clinical outcome of catheter ablation for persistent atrial fibrillation, Journal of the American College of Cardiology 54 (9) (2009) 788–795.
[40] R. Alcaraz, J.J. Rieta, A novel application of sample entropy to the electrocardiogram of atrial fibrillation, Nonlinear Analysis: Real World Applications 11 (2010) 1026–1035.
[41] M. Haïssaguerre, P. Jaïs, D. Shah, et al., Spontaneous initiation of atrial fibrillation by ectopic beats originating in the pulmonary veins, New England Journal of Medicine 339 (1998) 659–665.
[42] P.G. Platonov, I. Nault, F. Holmqvist, M. Stridh, M. Hocini, M. Haïssaguerre, Left atrial appendage activity translation in the standard 12-lead ECG, Journal of Cardiovascular Electrophysiology 22 (2011) 706–710.
[43] L.W. Lo, C.T. Tai, Y.J. Lin, et al., Predicting factors for atrial fibrillation acute termination during catheter ablation procedures: implications for catheter ablation strategy and long-term outcome, Heart Rhythm 6 (2009) 311–318.
[44] M. Holm, S. Pehrson, M. Ingemansson, et al., Non-invasive assessment of the atrial cycle length during atrial fibrillation in man: introducing, validating and illustrating a new ECG method, Cardiovascular Research 38 (1998) 69–81.

Please cite this article in press as: M. Meo, et al., Catheter ablation outcome prediction in persistent atrial fibrillation using weighted principal component analysis, Biomed. Signal Process. Control (2013), http://dx.doi.org/10.1016/j.bspc.2013.02.002